Critical behavior and synchronization of discrete stochastic phase coupled oscillators

Kevin Wood[1,2], C. Van den Broeck[3], R. Kawai[4], and Katja Lindenberg[1]
(1) *Department of Chemistry and Biochemistry and Institute for Nonlinear Science, University of California San Diego, 9500 Gilman Drive, La Jolla, CA 92093-0340, USA*
(2) *Department of Physics, University of California San Diego, 9500 Gilman Drive, La Jolla, CA 92093-0340, USA*
(3) *Hasselt University, Diepenbeek, B-3590 Belgium*
(4) *Department of Physics, University of Alabama at Birmingham, Birmingham, AL 35294 USA*
(Dated: February 5, 2008)

Synchronization of stochastic phase-coupled oscillators is known to occur but difficult to characterize because sufficiently complete analytic work is not yet within our reach, and thorough numerical description usually defies all resources. We present a discrete model that is sufficiently simple to be characterized in meaningful detail. In the mean field limit, the model exhibits a supercritical Hopf bifurcation and global oscillatory behavior as coupling crosses a critical value. When coupling between units is strictly local, the model undergoes a continuous phase transition which we characterize numerically using finite-size scaling analysis. In particular, we explicitly rule out multistability and show that that the onset of global synchrony is marked by signatures of the XY universality class. Our numerical results cover dimensions $d = 2$, 3, 4, and 5 and lead to the appropriate XY classical exponents β and ν, a lower critical dimension $d_{lc} = 2$, and an upper critical dimension $d_{uc} = 4$.

PACS numbers: 64.60.Ht, 05.45.Xt, 89.75.-k

I. INTRODUCTION

The role of dissipative structures and self-organization in systems far from equilibrium in the description of real and observable physical phenomena has been undisputed since the experiments with the Belusov-Zhabotinsky reactions in the early 1960's. The breaking of time translational symmetry has since become a central and typical theme in the analysis of nonlinear nonequilibrium systems. It is somewhat surprising that in the later studies of spatially distributed systems, most of the interest shifted to pattern forming instabilities, and little attention was devoted to the phenomenon of bulk oscillation and the required spatial frequency and phase synchronization, especially in view of the intense interest generated in the scientific and even broader community by the emergence of phase synchronization in populations of globally coupled phase oscillators [1]. The synchronous firing of fireflies is one of the most visible and spectacular examples of phase synchronization. Because intrinsically oscillating units with slightly different eigenfrequencies underlie the macroscopic behavior of an extensive range of biological, chemical, and physical systems, a great deal of literature has focused on the mathematical principles governing the competition between individual oscillatory tendencies and synchronous cooperation [2, 3, 4]. While most studies have focused on globally coupled units, leading to a mature understanding of the mean field behavior of several models, relatively little work has examined populations of oscillators in the locally coupled regime [5, 6, 7]. In fact, models of locally coupled oscillators typically involve a prohibitively large collection of interdependent nonlinear differential equations, thus preventing any extensive characterization of the phase transition to phase synchrony. Further inclusion of stochastic fluctuations in such models typically renders them computationally and analytically intractable for even a modest number of units. As a result, the description of emergent synchrony has largely been limited to small-scale and/or globally-coupled deterministic systems [8, 9], despite the fact that the dynamics of the physical systems in question likely reflect a combination of finite-range forces and stochasticity. Two recent studies by Risler et al. [10, 11] represent notable exceptions to this trend. Using an elegant renormalization group approach, they provide analytical evidence that identical locally-coupled noisy oscillators belong to the XY universality class, though to date there had been no empirical verification, numerical or otherwise, of their predictions.

The difficulty with existing models of locally coupled oscillators is that each is typically described by a nonlinear differential equation, and the resulting systems of coupled equations are computationally extravagant, especially when stochastic components are also included. Here we introduce a far more tractable model consisting

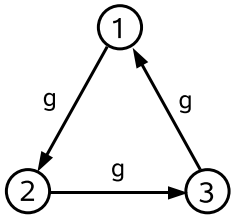

FIG. 1: Single three state unit with generic transition rates g.

of *identical* and *discrete* phase-coupled oscillators whose simple structure renders it amenable to extensive numerical study. The use of such minimal models is common in statistical physics, where microscopic details can often be disregarded in favor of phenomenological macroscopic variables. As Landau theory [12] reminds us, macroscopically observable changes (those that occur on length and time scales encompassing a magnificently large number of degrees of freedom) occur without reference to microscopic specifics. In a sense, the distinguishing features of even highly diverse systems become irrelevent for the description of cooperative behavior at the level of a phase transition; instead, the underlying statistical similarities give rise to classes of universal behavior whose members differ greatly at the microscopic level. In the spirit of this universality, simple toy models have been devised in hopes of capturing the essential qualitative features of phase transitions without concern for the microscopic structure of the problem. With this in mind, we construct the simplest model that exhibits global phase synchrony and contains the physical ingredients listed above, namely, stochastic variation within individual units and short-ranged interactions [13]. The simplicity of the model allows for relatively fast numerical simulation and thus an extensive description of the phase transition in question. An abbreviated version of our principal results can be found in [13]. There we characterized the universality class of the transition, including the critical exponents and the lower and upper critical dimensions. Here we present considerably more detail as well as additional results to support our characterization.

The organization of the paper is as follows. In Sec. II we introduce our description of a single unit as well as the coupling scheme between units. Section III presents the linear stability analysis of the mean field limit, and Sec. IV contains the finite-size scaling analysis that unveils the critical behavior of the locally-coupled model. We conclude with a summary in Sec V.

II. THREE STATE MODEL

Our starting point is a three-state unit [14] governed by transition rates g, as shown in Fig. 1. We interpret the state designation as a generalized (discrete) phase, and the transitions between states, which we construct to be unidirectional, as a phase change and thus an oscillation of sorts. The probability of going from the current state i to state $i+1$ in an infinitesimal time dt is gdt, with $i = 1, 2, 3$ modulo 3. For a single unit, g is simply a constant that sets the oscillator's intrinsic frequency; for many units coupled together, we will allow g to depend on the neighboring units in the spatial grid, thereby coupling neighboring phases. The choice of coupling, specified below, is not unique.

For a single unit we write the linear evolution equation

$$\frac{\partial}{\partial t}P(t) = MP(t) \tag{1}$$

where

$$P(t) = \begin{pmatrix} P_1(t) \\ P_2(t) \\ P_3(t) \end{pmatrix}, \tag{2}$$

$P_i(t)$ is the probability of being in state i at time t, and

$$M = \begin{pmatrix} -g & 0 & g \\ g & -g & 0 \\ 0 & g & -g \end{pmatrix}. \tag{3}$$

The system clearly reaches a steady state for $P_1^* = P_2^* = P_3^* = 1/3$. The transitions $1 \to 2$, $2 \to 3$, $3 \to 1$ occur with a rough periodicity determined by g. The time evolution of our simple model thus qualitatively resembles that of the discretized phase of a generic noisy oscillator.

We are interested in the behavior that emerges when individual units are coupled to one another by allowing the transition probability of a given unit to depend on the states of the unit's nearest neighbors in the spatial grid. The phase at a given site is compared with those of its neighbors, and the phase of the given site is adjusted so as to facilitate phase coherence. The expectation is to capture the physical nature of synchronization. It is further expected that within certain restrictions (e.g., the coupling must surely be nonlinear), the specific nature of the coupling is not important (in other words, we expect universality) so long as we ultimately observe a transition to global synchrony at some finite value of the coupling parameter. We settle upon a particular exponential form below. As we shall see, linear stability analysis for this choice confirms the existence of a Hopf bifurcation in the mean field limit.

More concretely, we specify that each unit may transition to the state ahead or remain in its current state depending on the states of its nearest neighbors. For unit μ, which we take to be in state i, we choose the transition rate to state j as follows:

$$g_{ij} = g \exp\left[\frac{a(N_j - N_i)}{2d}\right] \delta_{j,i+1}, \tag{4}$$

where a is the coupling parameter, δ is the Kronecker delta, N_k is the number of nearest neighbors in state k, and $2d$ is the total number of nearest neighbors in d dimensions. The transition rate is thus determined by the number of nearest neighbors of unit μ that are one state ahead and in the same state as unit μ. Table I shows the explicit transition rates in one dimension. While these rates are somewhat distorted by their assumed independence of the number of nearest neighbors in state $i-1$ (e.g. in one dimension the transition rate from state i to state $i+1$ is the same if both nearest neighbors are in state $i-1$ and if one is in state i and the other in $i+1$),

the form (4) is simplified by this assmumption and, as we shall see, does lead to synchronization. Note also that an equally simple model might posit a coupling which depends on N_{i-1}, the number of units 'behind' the unit in question, rather than N_{i+1}, or a more complex model could be constructed that depends on both. We settle on our choice (4) because the phase transition we seek occurs for a smaller value of the coupling constant a, and therefore numerical simulations can be run with larger time steps. We stress again that universality suggests that such microscopic details should not substantially alter the qualitative picture of the phase transition as long as the coupling is sufficiently nonlinear and favors synchronization.

III. MEAN-FIELD THEORY

To test for the emergence of global synchrony, we first consider a mean field version of the model, that is, one where each unit is coupled to all other units. In the large N limit with all-to-all coupling we write

$$g_{ij} = g \exp\left[a(P_j - P_i)\right] \delta_{j,i+1}, \tag{5}$$

where P_k is the (ensemble) probability of being in state k. Note that with all-to-all coupling g_{ij} does not depend on the location of the unit within the lattice. Note also that there is an inherent assumption that we can replace N_k/N with P_k, that is, we are assuming that N, the total number of units, is large enough that N_k/N serves as a good estimation of the ensemble probability P_k. With this simplification we arrive at an equation for the mean field P:

$$\frac{\partial}{\partial t} P(t) = M[P(t)]P(t), \tag{6}$$

where

$$M[P(t)] = \begin{pmatrix} -g_{12} & 0 & g_{31} \\ g_{12} & -g_{23} & 0 \\ 0 & g_{23} & -g_{31} \end{pmatrix}. \tag{7}$$

Neighbors	Transition Rate
$i-1,\, i-1$	g
$i-1,\, i$	$g\exp(-a/2)$
$i-1,\, i+1$	$g\exp(a/2)$
$i,\, i-1$	$g\exp(-a/2)$
$i,\, i$	$g\exp(-a)$
$i,\, i+1$	g
$i+1,\, i-1$	$g\exp(a/2)$
$i+1,\, i$	g
$i+1,\, i+1$	$g\exp(a)$

TABLE I: Transition rates in one dimension.

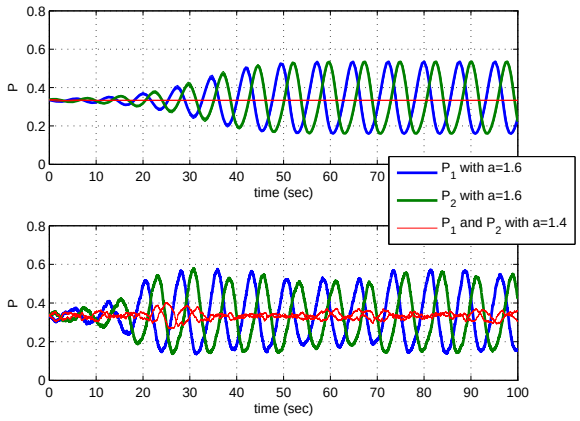

FIG. 2: Simulations with 5000 globally coupled units (bottom panel) agree well with the numerical solution of the mean field equations (top panel). As predicted by linearization, a Hopf bifurcation occurs near $a = 1.5$.

We have explicitly noted the dependence of M on $P(t)$ since each of the matrix elements g_{ij} depends on the evolving probabilities. Equation (6) is thus a highly nonlinear equation.

The normalization condition $P_1+P_2+P_3 = 1$ allows us to eliminate P_3 and obtain a closed set of equations for P_1 and P_2. We can further characterize the mean field solutions using standard linear stability analysis. Specifically, we linearize about the fixed point $(P_1^*, P_2^*) = (1/3, 1/3)$

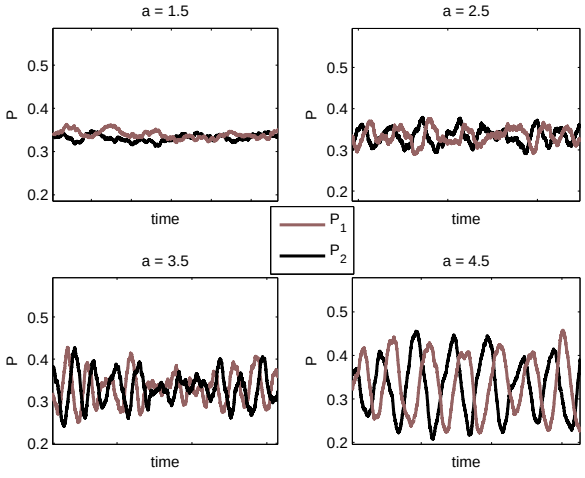

FIG. 3: Absence of synchronization in $2D$. Top left: $a = 1.5$. Top right: $a = 2.5$. Bottom left: $a = 3.5$. Bottom right: $a = 4.5$. $L = 100$ for all plots. Even for very large values of the coupling, highly synchronous oscillatory behavior is not present. As discussed in the text and shown in the next figure, the intermittent oscillations apparent for high values of a result from finite size effects.

and obtain the Jacobian J evaluated at (P_1^*, P_2^*):

$$J = \begin{pmatrix} ag - 2g & -g \\ g & ag - g \end{pmatrix}. \tag{8}$$

The eigenvalues of J characterize the fixed point, and they are given by:

$$\lambda_\pm = \frac{g}{2}(2a - 3 \pm i\sqrt{3}). \tag{9}$$

Both cross the imaginary axis at $a = 1.5$, indicative of a Hopf birfurcation at this value. Hence, as a increases the mean field undergoes a qualitative change at $a = 1.5$ from disorder ($P_1 = P_2 = P_3$) to global oscillations, and the desired global synchrony emerges.

The predictions of the linearization can be verified by numerically solving the mean field equations (6). In turn, these solutions agree well with direct simulations of the multiple unit model characterized by Eq. (4) if we consider all-to-all coupling rather than merely nearest-neighbor coupling (Fig. 2). As such, the mean field equations accurately capture the behavior of the nearest neighbor model in the high (spatial) dimensional limit.

Furthermore, the Hopf bifurcation seen in our mean field model can be shown to be supercritical. Such an analytical argument is formally related to the structure of the normal form for the Hopf bifurcation. Practically speaking, one must consider the sign of the first Lyapunov coefficient at the bifurcation point ($a_c = 1.5$). Following [15], we transform our two dimensional nonlinear equation (6) to a single equation for the complex variable z valid for small $\alpha = a - a_c$. The form of the equation is given by

$$\dot{z} = \lambda(\alpha)z + f(z, z^\dagger, \alpha), \tag{10}$$

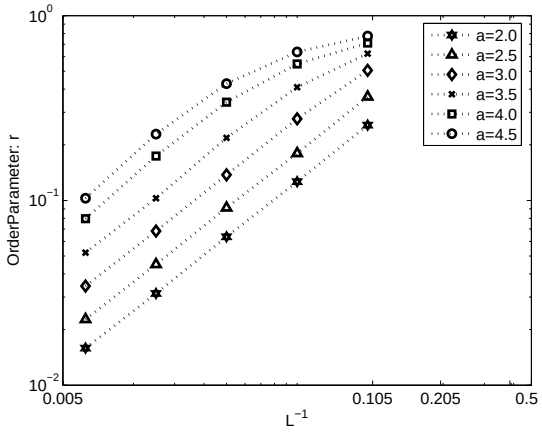

FIG. 4: Log-log plot of r vs L^{-1} for $d = 2$. The order parameter r tends to 0 as system size increases, verifying the absence of a transition in two dimensions. Even for large values of the coupling, synchronous oscillations die away in the limit of infinite system size.

where $f(z, z^\dagger, \alpha)$ is an $O(|z|^2)$ smooth function of z, $z^\dagger$, and α, and $\lambda(\alpha)$ is an α-dependent eigenvalue of the linearized Jacobian (8) given above. We achieve such a transformation by first finding complex eigenvectors p and q given by

$$J(0)q = \lambda(0)q, J(0)^T p = \lambda(0)^\dagger p, \tag{11}$$

with $J(0)$ the Jacobian evaluated at $a = a_c = 1.5$. One then normalizes $\langle p, q\rangle$, where brackets in this context represent the standard complex scalar product. An equation for z of the desired form (10) is formally attained at $\alpha = 0$ as

$$\dot{z} = \lambda(0)z + \langle p, F(zq + z^\dagger q^\dagger, 0)\rangle, \tag{12}$$

where $F(x, \alpha)$ is related to our original dynamical system, i.e.,

$$\frac{\partial}{\partial t}P(t) = J(\alpha)P(t) + F[P(t), \alpha]. \tag{13}$$

From this, we may obtain the first Lyapunov coefficeint L_1 as

$$L_1 = \frac{1}{2\omega_0^2} Re(if_{20}f_{11} + w_0 f_{21}), \tag{14}$$

with f_{ij} given by the formal Taylor expansion of f,

$$f(z, z^\dagger, 0) = \langle p, F(zq + z^\dagger q^{dag}, 0)\rangle = \sum_{k+l\geq 2} \frac{1}{k!l!} f_{kl} z^k (z^\dagger)^l. \tag{15}$$

An explicit calculation for our mean field dynamical system reveals that $L_1 < 0$, indicative of a supercritical Hopf bifurcation to a unique, stable limit cycle as a eclipses a_c.

In what follows, we characterize the breakdown of the mean field description as spatial dimension is decreased, and characterize the phase transitions observed with nearest-neighbor coupling.

IV. CRITICAL BEHAVIOR OF THE LOCALLY COUPLED MODEL

With a firm understanding of the mean field model, we now follow with a study of the locally coupled model. We perform simulations in continuous time on d-dimensional cubic lattices of various sizes. For all simulations, we implement periodic boundary conditions. Time steps dt are taken to be 10 to 100 times smaller than the fastest possible local average transition rate, that is, $dt \ll e^{-a}$ (we set $g = 1$ in our simulations). This estimate is actually quite conservative, particularly because the fastest possible transition corresponds to a single unit in state i with all $2d$ nearest neighbors in state $i + 1$, a scenario which certainly does not dominate the macroscopic dynamics. We have ascertained that differences between these simulations and others run at much smaller time steps (500 to 1000 times smaller than e^{-a}) are very small. All

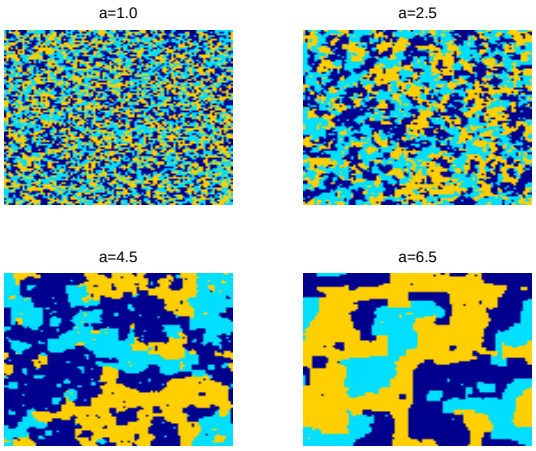

FIG. 5: Snapshots of the system in $d = 2$ are shown for $a = 1$, $a = 2.5$, $a = 4.5$, and $a = 6.5$. Upon close inspection, one can discern vortex-like structures, particularly for the higher values of a. The three colors represent units in the three possible states.

simulations were run until an apparent steady state was reached. Furthermore, we start all simulations from random initial conditions, and we calculate statistics based on 100 independent trials. Although the simplicity of the model allows for efficient numerical simulation, our results nevertheless represent a modest computational achievement; simulations required approximately 5 weeks on a 28-node dual processor cluster.

To characterize the emergence of phase synchrony, we introduce the order parameter [8]

$$r = \langle R \rangle, \qquad R \equiv \frac{1}{N} |\sum_{j=1}^{N} e^{i\phi_j}|. \tag{16}$$

Here ϕ is a discrete phase, taken to be $2\pi(k-1)/3$ for state $k \in \{1, 2, 3\}$ at site j. The brackets represent an average over time in the steady state and an average over all independent trials. A nonzero value of r in the thermodynamic limit signifies the presence of synchrony. We also make use of the corresponding generalized susceptibility

$$\chi = L^d[\langle R^2 \rangle - \langle R \rangle^2]. \tag{17}$$

We begin by considering the model in two spatial dimensions. Here, as shown in Fig. 3, we do not see the emergence of global oscillatory behavior. Instead, we observe intermittent oscillations (for very large values of a) that decrease drastically with increasing system size. In fact, as depicted in Fig. 4, r approaches zero in the thermodynamic limit, even for very large values of a. We conclude that the phase transition to synchrony cannot occur for $d = 2$. Interestingly, snapshots of the sytem reveal increased spatial clustering as a is increased as well as the presence of defect structures, perhaps indicative of Kosterlitz-Thouless-type phenomena (Fig. 5) [12]. Further studies along these lines are underway.

In contrast to the $d = 2$ case, which serves as the lower critical dimension, a clear thermodynamic-like phase transition occurs in three spatial dimensions. We see the emergence of global oscillatory behavior, which persists in the limit of large system size, as a increases past a critical value a_c (Figs. 6 and 7). This is consistent with the predictions of the mean field theory. For $a < a_c$, r approaches zero as system size is increased, and a disordered phase persists in the thermodynamic limit. As expected, for $a > a_c$ the steady state dynamics of P_1 and P_2 exhibit smooth temporal oscillations (see the lower insets in Fig. 7) similar to the mean field case beyond the Hopf bifurcation point. In addition, Fig. 7 shows the behavior of the order paramater as a is increased for the largest system studied ($L = 80$); the upper left inset shows the peak in χ at $a = 2.345 \pm 0.005$, thus providing an estimate of the critical point a_c where fluctuations are largest. Strictly speaking, we must extrapolate this peak to obtain a result in the limit of infinite system size, but we see no change as system size is increased beyond $L = 40$, indicating that finite size effects are small in systems beyond this size. At any rate, such finite size effects are within the range of our estimation. We tried to apply the Binder cumulant crossing method [16] for determining a_c more precisely, but residual finite size effects and statistical uncertainties in the data prevent us from determining the crossing point with more precision than that stated above. In any case, we are only interested in determining the critical point with sufficient accuracy to determine the universality class of the transition. For this, as we show below, our current estimation suffices in three dimensions as well as in higher dimensions. In

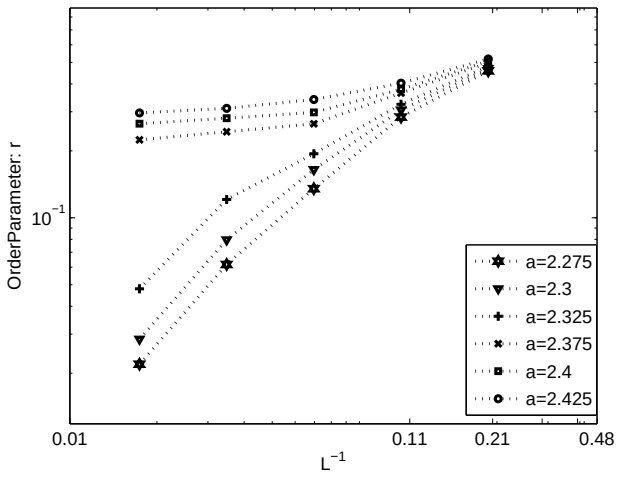

FIG. 6: Log-log plots of r vs L^{-1} for $d = 3$. For $a > a_c$, the order parameter r approaches a finite value, even as the system size increases indefinitely. For $a < a_c$, r approaches zero in the thermodynamic limit.

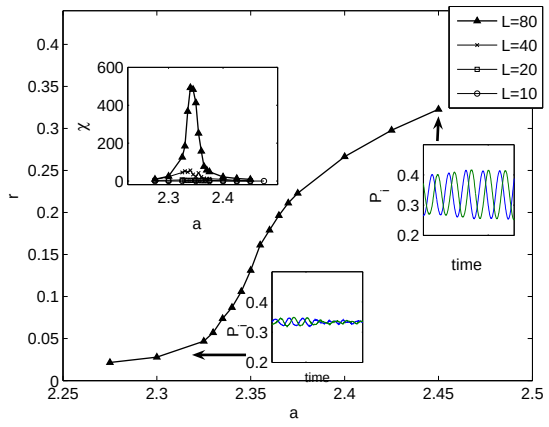

FIG. 7: Onset of synchronization in $d = 3$. Global oscillatory behavior emerges as a is increased beyond a_c, as indicated by the increasing value of r. The system size is $L = 80$. Upper left inset: Fluctuations peak near the critical point, giving an estimation of $a_c = 2.345 \pm 0.005$. Right insets: P_1 and P_2 undergo smooth temporal oscillations for large a (upper right), while a lower value of a decreases temporal coherence (lower left).

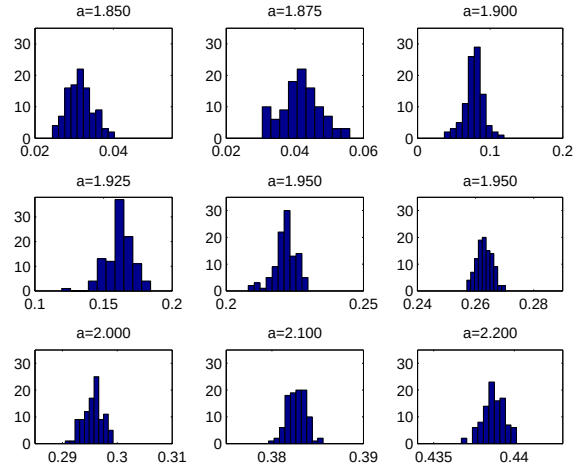

FIG. 8: Lack of multistability in $d = 4$: Histograms over all independent trials show only single peaks of varying widths, consistent with the expectations for a second order phase transition.

addition, we note that the transiition to synchrony appears to be a smooth, second order phase transition. To rule out potential multistability (and thus a discontinuous first order transition), we show histograms of r for $d = 4$ given over all independent trials in Fig. 8. The histograms show no evidence whatsoever of multiple peaks beyond the statistical fluctuations expected for the relatively small sample size, and thus we can safely rule out a discontinuous transition, in agreement with the findings of the mean field analysis. Similarly peaked histograms are found in $d = 3$ (less sharply peaked but distinctly unimodal) and $d = 5$ (more sharply peaked).

To further characterize this transition, we use a systematic finite size scaling analysis. We start by assuming the standard form for r in a finite system,

$$r = L^{-\frac{\beta}{\nu}} F[(a - a_c)L^{\frac{1}{\nu}}], \tag{18}$$

where $F(x)$ is a scaling function that approaches a constant as $x \to 0$. This ansatz suggests that near the critical point we should plot $rL^{\frac{\beta}{\nu}}$ vs. $(\frac{a}{a_c} - 1)L^{\frac{1}{\nu}}$, and data from different system sizes should collapse onto a single curve. To test our numerical data against different universality classes we choose the appropriate critical exponents for each, recognizing that there are variations in the reported values of these exponents. For the XY universality class we use the exponents reported in [17] ($\beta = 0.34$ and $\nu = 0.66$). For the Ising exponents we use those given in [18] ($\beta = 0.31$ and $\nu = 0.64$). In Fig. 9, we see quite convincingly a collapse when exponents from the XY class are used. For comparison, we also show the data collapse when 3D Ising exponents are used (Fig. 10). Our data suggests that the model falls within the XY

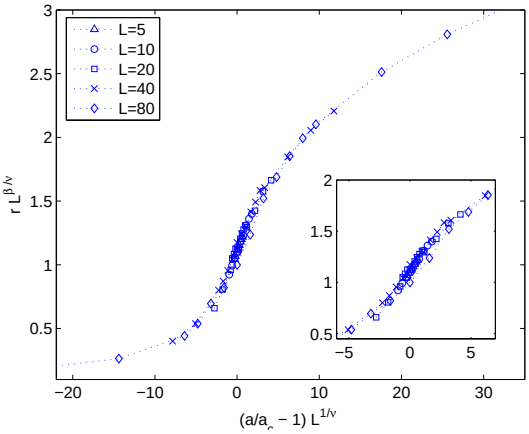

FIG. 9: Exponents in $d = 3$: Data collapse of $rL^{\frac{\beta}{\nu}}$ vs $(a/a_c - 1)L^{\frac{1}{\nu}}$. With $a_c = 2.345$, we show the data collapse using the theoretical XY exponents in $3D$. The collapse is excellent, suggesting that the model is in the XY universality class. The insets show a closer view near the critical point.

Universality class, though the very small differences between XY and Ising exponents makes it impossible to entirely rule out Ising-like behavior. We should point out that while some reported values of the Ising critical exponents differ from the XY values by more than those used above, others differ by less (see [19] for an exhaustive collection of estimates). Note that this scaling procedure was attempted for many values a_c within the stated range of accuracy. In all cases where a distinction could be made, the XY exponents provided a better collapse than the corresponding Ising exponents.

To complete the analogy with the equilibrium phase transition, we explore spatial correlations in $d = 3$.

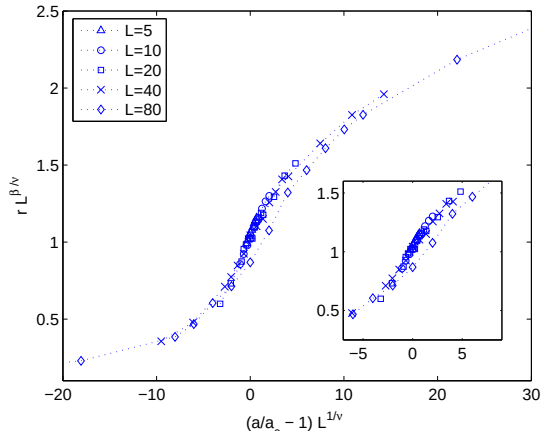

FIG. 10: Exponents in $d = 3$. Data collapse of $rL^{\frac{\beta}{\nu}}$ vs $(a/a_c - 1)L^{\frac{1}{\nu}}$. With $a_c = 2.345$, we show the data collapse using theoretical Ising 3D exponents. The collapse is reasonable good, but still poor compared with that seen with exponents from the XY class. Insets show a closer view near the critical point.

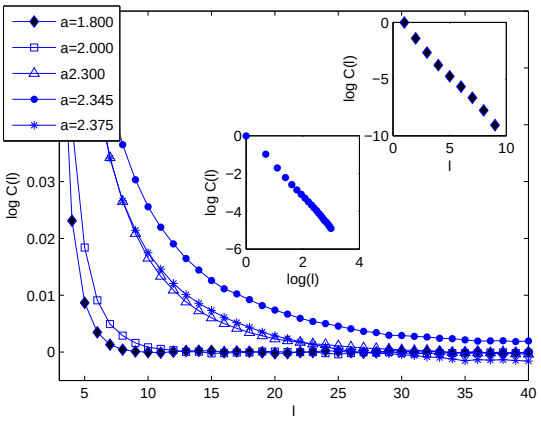

FIG. 11: Spatial correlations in $d = 3$. As a approaches the critical value a_c, evidence of long range correlations develops, indicative of a diverging correlation length at the critical point. The lower inset shows the power law decay of the correlation function at the critical point, while the upper inset shows that the correlation function decays exponentially far from the critical point.

Specifically, we calculate $C(l)$, the spatial correlation function, given by

$$C(l) = \langle \sum_{j=1}^{N} \sum_{n=1}^{3} \exp(i\phi_j) \exp(-i\phi_{j+l_n}) \rangle - r^2. \qquad (19)$$

Here ϕ_j again indicates the discrete phase of the oscillator at site j, and l_n denotes the Cartesian components in the x, y, and z directions at distance l from site j. The correlation function depends only on this distance. As seen in Fig. 11, correlations develop for values of a near the critical point, while this correlation is absent away from a_c. The functional form of $C(l)$ as a approaches a_c is similar to that seen in equilibrium transitions. Indeed, the lower inset is at the critical point ($a = 2.345$) and explicitly shows power law decay of the correlation function. The upper inset is far from the critical point ($a = 1.8$) and shows exponential decay.

In four spatial dimensions we also see a transition to synchrony characterized by large fluctuations at the critical point. Here we estimate the transition coupling to be $a_c = 1.900 \pm 0.025$ by again considering the peak in χ (see Figs. 12 and 13). Because we expect $d = 4$ to be the upper critical dimension in accordance with XY/Ising behavior, we anticipate a slight breakdown of the scaling relation (18). An alternate scaling ansatz valid at d_{uc} is given by (18) with the transformation $L \to ln(L)L^{1/4}$ [20]. A priori it is not clear how strongly (18) will be violated in $d = 4$, nor is it clear that the modified ansatz will better serve our purposes; therefore, we will use both forms of scaling in testing for the mean field exponents $\nu = 1/2$ and $\beta = 1/2$.

As shown in Fig. 14, the data collapse is very good with the mean field exponents regardless of which scaling ansatz is used. As such, our simulations suggest that

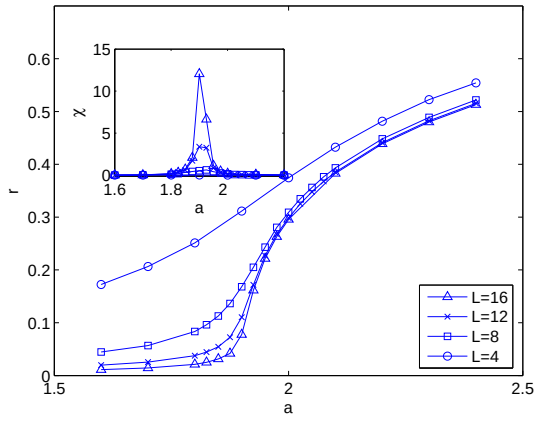

FIG. 12: Transition in $d = 4$: The behavior of the order parameter near the transition point is shown for various system sizes. The inset shows the generalized susceptablitiy, χ, which peaks at $a = 1.900 \pm 0.025$, giving an estimation of a_c.

$d = 4$ serves as the upper critical dimension; additionally, it appears that corrections to finite-size scaling at $d = 4$ are not substantial, though a much more precise study would be needed to investigate such corrections in greater detail.

To further support the claim that $d_{uc} = 4$, we consider the case $d = 5$. We see a transition to synchrony which occurs at $a_c = 1.750 \pm 0.015$ (see Figs. 15 and 16). As expected, this value for a_c is considerably closer than the critical coupling in four dimensions to the value $a_c = 1.5$ calculated by linear stability analysis in mean field theory.

Finally, it is interesting to test the suggestion of Jones

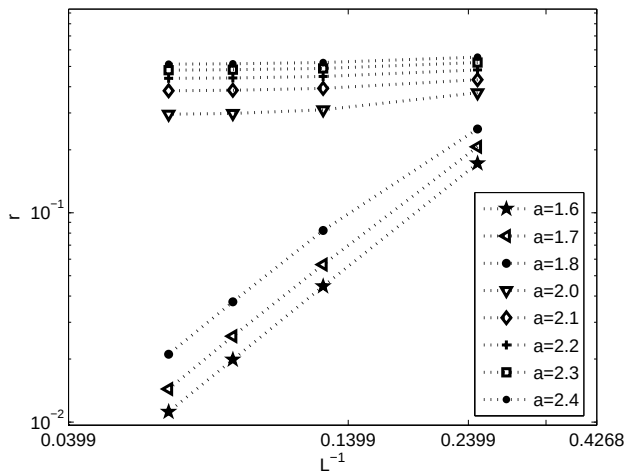

FIG. 13: Log-log plots of r vs L^{-1} for $d = 4$. The order parameter r clearly approaches a finite, nonzero value for $a > a_c$ and approaches 0 for $a < a_c$.

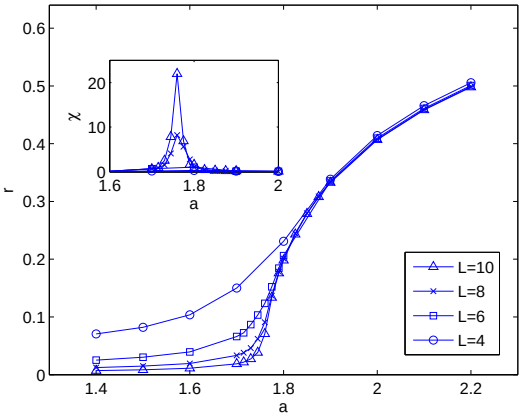

FIG. 15: Transition in $d = 5$: The behavior of the order parameter near the transition point is shown for various system sizes. The inset shows the generalized susceptibility, χ, which peaks at $a = 1.750 \pm 0.015$, giving an estimation of a_c.

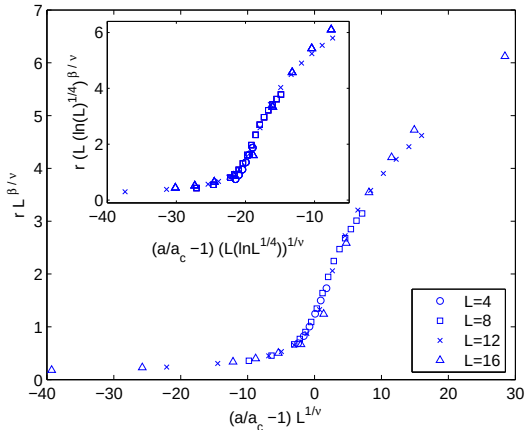

FIG. 14: Exponents in $d = 4$: Data collapse of original ansatz (18) with mean field exponents. Inset: Data collapse with modified scaling ansatz $r(\ln(L)L^{1/4})^{\frac{\beta}{\nu}}$ vs $(\frac{a}{a_c} - 1)(\ln(L)L^{1/4})^{\frac{1}{\nu}}$ with mean field exponents.

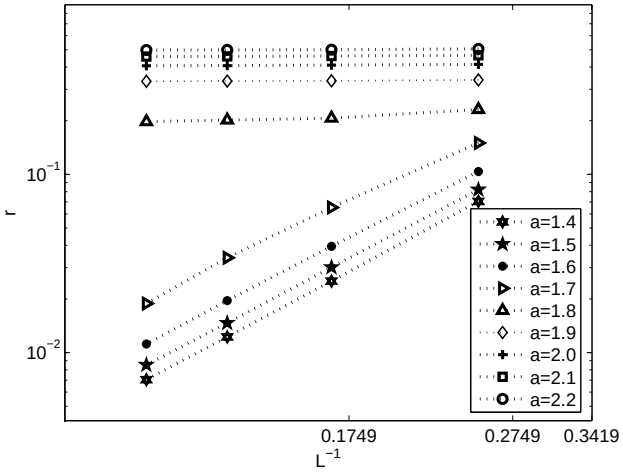

FIG. 16: Log-log plots of r vs L^{-1} in $d = 5$. The order parameter r clearly approaches a finite, nonzero value for $a > a_c$ and approaches 0 for $a < a_c$. The value of a_c appears to fall between $a = 1.8$ and $a = 1.7$.

and Young [20] that above the critical dimension, $d \geqslant d_{uc}$, it is appropriate to modify the finite size scaling ansatz (18) by the transformation $L \to L^{d/4}$. We test this suggestion for $d = 5$. As indicated in Fig. 17, the data collapse is excellent for both the original scaling and the modified form of the ansatz. The collapse of the data with mean field exponents seems slightly better using the modified ansatz, though a much more precise study would be required to accurately capture the form of the modified scaling in $d > d_{uc}$. In any case, our data suggest that the model exhibits mean field behavior in $d = 5$, verifying that $d = 4$ serves as the upper critical dimension.

V. SUMMARY

We have introduced a simple discrete model for studying phase coherence in spatially distributed populations of noisy coupled oscillators. This model lends itself to numerical study even in the case of nearest neighbor coupling because each oscillator is a simple three-state system rather than one of the usual continuum choices. The coupled system is therefore much simpler than the usual set of coupled nonlinear differential equations.

A mean field treatment combined with linear stability analysis shows that the globally coupled model undergoes a Hopf bifurcation to macroscopic synchrony as the coupling parameter a is increased. We are able to determine

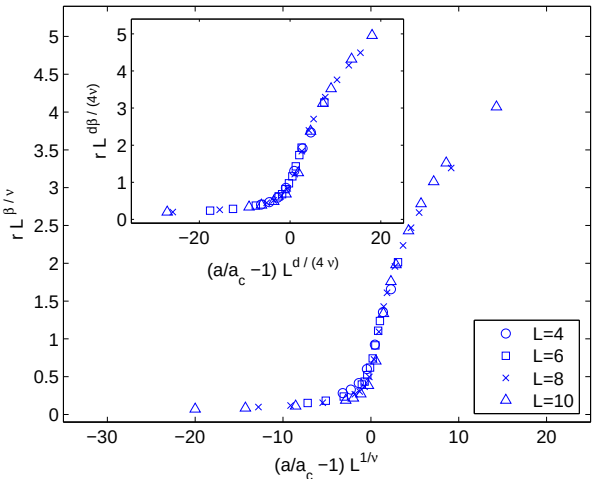

FIG. 17: Exponents in $d = 5$: Data collapse of original ansatz (18) with mean field exponents. Inset: Data collapse of $rL^{\frac{d\beta}{4\nu}}$ vs. $(a/a_c - 1)L^{\frac{d}{4\nu}}$ with mean field exponents. The collapse of the data is quite convincing when the exact mean field exponents are used.

the mean field critical coupling constant analytically. For locally coupled units, numerical solution of the system shows the emergence of a thermodynamic synchronous phase for $d > 2$, indicating that the lower critical dimension is $d_{lc} = 2$. As d is increased, the numerically established critical value a_c approaches that predicted by the mean field treatment of the model. For $d = 3$, we give strong numerical evidence that the model falls into the 3D XY universality class, while for $d = 4$ the critical exponents are those predicted by mean field theory. The exponents in $d = 5$ also take on the mean field values, thus verifying that $d = 4$ corresponds to the upper critical dimension d_{uc}.

In conclusion, while nonequilibrium phase transitions have a much wider diversity in universality classes than equilibrium ones [21], it is remarkable that the prototype of a nonequilibrium transition, namely, a phase transition that breaks the symmetry of translation in time, is described, at least for the critical exponents investigated in this paper, by an equilibrium universality class. In particular, the Mermin-Wagner theorem, stating that continuous symmetries can not be broken in dimension two or lower, appears to apply. Furthermore, the XY model is known to display a Kosterlitz-Thouless transition, in which, beyond a critical temperature, vortex pairs can unbind into individual units creating long range correlations. Preliminary results indicate that a similar transition occurs in our model. Finally, a note of caution concerning the discreteness of the phase is in order. We first note that microscopic models often feature discrete degrees of freedom. For example, our model is reminiscent of the triangular reaction model introduced by Onsager [22], on the basis of which he illustrated the concept of detailed balance as a characterization of equilibrium. Continuous phase models appear in a suitable thermodynamic limit. We stress that the breaking of time translational symmetry can occur independently of whether the phase is a discrete or continuous variable. It is, however, not evident whether continuous and discrete phase models belong to the same universality class. The results found here seem to support the latter thesis, but a renormalization calculation confirming this hypothesis would be welcome.

Acknowledgments

This work was partially supported by the National Science Foundation under Grant No. PHY-0354937.

[1] S. H. Strogatz, *Nonlinear Dynamics and Chaos* (Westview Press, 1994).
[2] A. T. Winfree, J. Theor. Biol. **16**, 15 (1967).
[3] Y. Kuramoto, *Chemical Oscillations, Waves, and Turbulence* (Springer, Berlin, 1984).
[4] S. H. Strogatz, Physica D **143**, 1 (2000).
[5] H. Sakaguchi, S. Shinomoto, and Y. Kuramoto, Prog. Theor. Phys. **77**, 1005 (1987); H. Daido, Phys. Rev. Lett. **61**, 231 (1988); S. H. Strogatz and R. E. Mirollo, J. Phys. A **21**, L699 (1988); *idem*, Physica D **31**, 143 (1988); H. Hong, H. Park, and M. Choi, Phys. Rev. E **71**, 054204 (2004).
[6] D. Walgraef, G. Dewel, and P. Borckmans, J. Chem. Phys. **78**, 3043 (1983).
[7] M. Malek Mansour, J. Dethier, and F. Baras, J. Chem. Phys. **114**, 9265 (2001).
[8] H.Hong, H. Park, M. Choi, Phys. Rev. E **71**, 054204 (2004).
[9] A. Pikovsky, M. Rosenblum, J. Kurths, *Synchronization: A Universal Concept in Nonlinear Science* (Cambridge University Press, Cambridge, 2001).
[10] T. Risler, J. Prost, F. J ulicher. Phys. Rev. Lett. **93**, 175702 (2004).
[11] T. Risler, J. Prost, and F. J ulicher, Phys. Rev. E **72**, 016130 (2005).
[12] N. Goldenfeld, *Lectures on Phase Transitions and the Renormalization Group* (Westview Press, 1992).
[13] K. Wood, C. Van den Broeck, R. Kawai, and K. Lindenberg, Phys. Rev. Lett. **96**, 145701 (2006).
[14] T. Prager, B. Naundorf, and L. Schimansky-Geier, Physica A **325**, 176 (2003).
[15] Y.A. Kuznetsov, *Elements of Applied Bifurcation Theory*, 2nd ed. (Springer, New York, 1998).
[16] K. Binder, Z. Phys. B **43**, 119 (1981).
[17] A. P. Gottlob and M. Hasenbusch, Nucl. Phys. B Suppl. **30**, 838 (1993).

[18] K. Huang, *Statistical Mechanics* Second Edition (Wiley, New York, 1988).
[19] A. Pelissetto and E. Vicari, Phys. Rep. **368**, 549 (2002).
[20] J. Jones and A. Young, Phys. Rev. B **71**, 174438 (2005).
[21] See, e.g., J. Marro and R. Dickman, *Nonequilibrium Phase Transitions in Lattice Models* (Cambridge University Press, Cambridge, 1999) and references therein; V. Privman, *Nonequilibrium Statistical Mechanics in One Dimension* (Cambridge University Press, Cambridge, 1997).
[22] L. Onsager, Phys. Rev. **37**, 405; *ibid*, Phys. Rev. **38** 2265(1931).